F4-TCNQ concentration dependence of the current–voltage characteristics in the Au/P3HT:PCBM:F4-TCNQ/n-Si (MPS) Schottky barrier diode

E. Yağlıoğlu and Ö. Tüzün Özmen[†]

Department of Physics, Faculty of Arts and Sciences, Düzce University, 81620 *Düzce, Turkey*

(Received 30 June 2014; revised manuscript received 25 July 2014; published online 20 October 2014)

In this study, we investigate some main electrical parameters of the gold/poly(3-hexylthiophene):[6,6]-phenyl C61 butyric acid methyl ester:2,3,5,6-tetrafluoro-7,7,8,8-tetracyanoquinodimethane/n-type silicon (Au/P3HT:PCBM:F4-TCNQ/n-Si) metal–polymer–semiconductor (MPS) Schottky barrier diode (SBD) in terms of the effects of F4-TCNQ concentration (0%, 1%, and 2%). F4-TCNQ-doped P3HT:PCBM is fabricated to figure out the p-type doping effect on the device performance. The main electrical parameters, such as ideality factor (n), barrier height (Φ_{B0}), series resistance (R_s), shunt resistance (R_{sh}), and density of interface states (N_{ss}) are determined from the forward and reverse bias current–voltage (I–V) characteristics in the dark and at room temperature. The values of n, R_s, Φ_{B0}, and N_{ss} are significantly reduced by using the 1% F4-TCNQ doping in P3HT:PCBM:F4-TCNQ organic blend layer, additionally, the carrier mobility and current are increased by the soft (1%) doping. The most ideal values of electrical parameters are obtained for 1% F4-TCNQ used diode. On the other hand, the carrier mobility and current for the hard doping (2%) become far away from the ideal diode values due to the unbalanced generation of holes/electrons and doping-induced disproportion when compared with 1% F4-TCNQ doping. These results show that the electrical properties of MPS SBDs strongly depend on the F4-TCNQ doping and doping concentration of interfacial P3HT:PCBM:F4-TCNQ organic layer. Moreover, the soft F4-TCNQ doping concentration (1%) in P3HT:PCBM:F4-TCNQ organic layer significantly improves the electrical characteristics of the Au/P3HT:PCBM:F4-TCNQ/n-Si (MPS) SBDs which enables the fabricating of high-quality electronic and optoelectronic devices.

Keywords: P3HT:PCBM:F4-TCNQ interfacial organic layer, F4-TCNQ doping concentration, Schottky barrier diodes, I–V characteristics

PACS: 73.40.Qv, 73.61.Ph, 81.05.Fb, 85.30.Hi **DOI:** 10.1088/1674-1056/23/11/117306

1. Introduction

In the last few decades, the polymeric organic materials have been a subject of intensive research, particularly in electronic devices.[1] Organic materials have been widely investigated due to their attractive applications in microelectronic and optoelectronic devices, such as organic field effect transistor (OFETs),[2] organic thin film transistors (OTFTs),[3] organic light emitting diodes (OLEDs),[4] Schottky diodes,[5] organic solar cells,[6] and organic photodetectors.[7] The advantages of polymeric organic materials, which include low-temperature processing, flexibility, low cost, good film forming properties, easy fabrication techniques, and large area processing, allow a variety of large application fields. Recently, electronic systems moved to the ultimate scale of molecular entities as demonstrated by the growing interest in understanding transport through polymeric organic molecules combining two metal contacts[8] and metal/polymeric organic material/semiconductor (MPS) structure.[9] Schottky barrier diodes (SBDs) are the most widely used diodes in electronic devices because of their low forward voltage drops, which allows lower power loss than ordinary silicon pn junction diodes. The properties of MPS SBDs are mainly controlled by their organic interfacial layer on semiconductor.

The optoelectronic devices with pure conjugated polymers have quite low device performances when compared with interpenetrating donor–acceptor networks.[10] Photodetectors and photovoltaic devices based on blends of conjugated polymers with fullerenes, forming interpenetrating donor–acceptor networks are a prototype application for the bulk heterojunction geometry.[11] Interpenetrating conjugated polymer:fullerene (donor–acceptor) networks defined as homogeneous blend of a p-type (donor) with an n-type semiconductor (acceptor) is a very promising approach to the improvement of the device performances. Interpenetrating conjugated polymer:fullerene (donor–acceptor) networks have larger interface area required for efficient exciton dissociation.[12] Charge transfer across a donor–acceptor interface provides an effective way to overcome early time-carrier recombination in an organic system and thus enhance its optoelectronic response.[10] Additionally, the poor electron mobility of n-type organic semiconductors compared with those of p-type counterparts can be enhanced using organic acceptors with high electron mobility such as fullerene.[12] The use of interpenetrating conjugated polymer:fullerene (donor–acceptor) networks instead of pure conjugated polymers gives rise to

[†]Corresponding author. E-mail: ozgetuzun@duzce.edu.tr

© 2014 Chinese Physical Society and IOP Publishing Ltd

ultrafast photo-induced charge transfer and charge separation with quantum efficiency approaching to unity, leaving holes in the donor phase and electrons in the acceptor phase due to the interfacial potential barrier that is responsible for the built-in potential in the donor–acceptor heterojunction devices.[10] Among polymer:fullerene (donor–acceptor) networks, the blend of poly(3-hexylthiophene) (P3HT) and [6,6]-phenyl C61 butyric acid methyl ester (PCBM) is promising and well-studied. This blend is usually used for photovoltaic devices due to its efficiency, which is as high as $\sim 6.5\%$.[13] P3HT, which is the pure conjugated polymer, has considerable applications in the electronic devices due to its high crystallinity and relatively high conductivity. To enhance the conducting polymer's capability to improve the charge collection under the operational bias and the quality of device, electron acceptors can be added. The P3HT electronic structure can be changed by adding a strong electron acceptor. PCBM, which is the fullerene, is known to be an excellent photoluminescence (PL) quencher when blended with P3HT.[14] Additionally, PCBM is one of the strong electron acceptors. The lowest unoccupied molecular orbital (LUMO) of PCBM is higher than the highest occupied molecular orbital (HOMO) of P3HT, which leads to incomplete charge transfer between PCBM and P3HT.[15]

The electrical characteristics of optoelectronic devices can be improved by using dopant molecules. Molecular doping process is quite critical in tuning the injection properties at metal–semiconductor interfaces, which leads to full control over device parameters.[16] Positioning of dopants in transport layers, which improves the charge injection by placing dopants near the contacts,[17] enhances carrier drift/diffusion and also charge separation at heterojunctions.[18] Therefore, the control of the electrical properties of diodes can be controlled by the molecular doping process.

Molecular doping is preferable for organic semiconductor devices, for the field-induced drift of the relative large-size charged molecular dopants can be suppressed.[19] To achieve the effective doping of P3HT, we use small molecule 2,3,5,6-tetrafluoro-7,7,8,8-tetracyanoquinodimethane (F4-TCNQ), which is known to be one of the most effective dopants for conjugated polymer:fullerene systems, resulting in p-type doping due to its strong electron affinity.[19] F4-TCNQ molecules easily accept the electrons from P3HT backbones to form charge-transfer complexes.[20] The charge-transfer complexes provide strong electrostatic force between P3HT and F4-TCNQ molecules which accelerates molecular orientation of the P3HT chain during electrical applications.[14] Additionally, the Fermi level of donor achieved by p-type doping (F4-TCNQ) also plays a critical role in charge transfer process which is dramatically enhanced by the intentional solution-based chemical doping of F4-TCNQ.[21] The F4-TCNQ demonstrated that doping leads to an increase not only in conductivity but also in mobility, which may result in the general improvement on the electrical properties in MPS SBDs through doping. Therefore, understanding the effects of F4-TCNQ dopant concentration on the electrical properties could be important to control the device performance.

By manipulating the F4-TCNQ concentration in the P3HT:PCBM:F4-TCNQ interfacial organic layer, the electrical properties of MPS SBDs can be developed when compared with those of only P3HT:PCBM interfacial organic layer used diode. Since the electrical properties of the junction govern the performance of the electronic device, the control of the nanoscale composition of the P3HT:PCBM:F4-TCNQ blend layer and the interface between metal/polymer (M/P) and polymer/semiconductor (P/S) are clearly important in the optimization of the performance of the structure.[22] Additionally, understanding the current control mechanisms for all samples with different F4-TCNQ doping concentrations in the interfacial organic layer can be very important to improve the device performances of MPS SBDs.

However, to the best of our knowledge, there is no report regarding the investigation of the F4-TCNQ doping effect on the performances of MPS SBDs. In this study, the effects of different F4-TCNQ doping concentrations on the electrical properties of the Au/P3HT:PCBM:F4-TCNQ/n-Si (MPS) SBDs are investigated. Various F4-TCNQ doping concentrations in a range of 0%–5% are used to fabricate the Au/P3HT:PCBM:F4-TCNQ/n-Si (MPS) SBDs. However, among all the diodes, the diodes doped with 0%, 1%, and 2% F4-TCNQ doping concentrations significantly show the effects of F4-TCNQ doping concentration on the electrical parameters of diodes. Current–voltage (I–V) measurements in the dark and at room temperature are carried out to figure out the basic electrical parameters of the Au/P3HT:PCBM:F4-TCNQ/n-Si (MPS) SBDs as functions of 0%, 1%, and 2% F4-TCNQ doping concentrations in P3HT:PCBM:F4-TCNQ interfacial organic layer respectively. The critical electrical parameters which determine the performances of the SBDs, i.e., the values of ideality factor (n), barrier height (Φ_{B0} and Φ_B), series resistance (R_s), shunt resistance (R_{sh}), electron mobility (μ_e), and the density of interface states (N_{ss}) at the metal/polymer (M/P) interfacial layer and polymer/semiconductor (P/S) interface, are obtained from the I–V analysis.

2. Experiment

2.1. Preparation of blend solution

The P3HT, PCBM, and F4-TCNQ organic compounds were purchased from Sigma-Aldrich Ltd. and used without further purification. The PCBM is a soluble form of fullerenes blended with conjugated polymers with nano-particles such as

C_{60}, while F4-TCNQ can be dissolved in organic solvents at elevated temperatures.[23]

Three concentrated solutions of P3HT (25 mg/mL), PCBM (25 mg/mL), and F4-TCNQ (0.01 mg/mL) were separately prepared in 1,2-dichlorobenzene and stirred at 60 °C for 3 h. Firstly, P3HT and PCBM were mixed to form the P3HT:PCBM blend solution with a weight ratio of 1:1 (10 mg/mL:10 mg/mL). Then, various amounts of F4-TCNQ solution were added into the P3HT:PCBM solution to obtain separate P3HT:PCBM solutions with the F4-TCNQ concentrations of 1% and 2% (wt-%). Subsequently, the blend solution was stirred overnight before spin casting for complete mixing. Additionally, the P3HT:PCBM blend solution without F4-TCNQ doping was fabricated as a reference of the undoped P3HT:PCBM (i.e., 0%) organic interfacial layer.

2.2. Schottky barrier diode fabrication

For the fabrication of the Au/P3HT:PCBM:F4-TCNQ/n-Si (MPS) SBDs with different F4-TCNQ doping concentrations, phosphorus-doped n-type single crystalline silicon (sc-Si) wafer (with ⟨100⟩ orientation, 350 ± 25-μm thick, 4.8-Ω·cm resistivity) was used as a substrate. The Si wafer was cleaned by using RCA cleaning procedure as described in Ref. [24]. Immediately, after the surface cleaning of sc-Si wafer, silver (Ag) metal with a thickness of ∼ 2500 Å, which was used as the low-resistivity ohmic back contact, was evaporated onto the whole back side of RCA-cleaned Si substrate by thermal evaporation system. Then, Ag-evaporated Si substrates were annealed by the thermal annealing at 450 °C for 30 min under N_2 flow in order to achieve a good ohmic contact. After the formation of the ohmic contact, the front side of the wafer was cleaned using 50% HF solution to remove the thin native oxide layer on the front side of the sc-Si wafer, which was formed in the ohmic contact formation processes.

Immediately, the P3HT:PCBM (1:1) solutions with F4-TCNQ concentrations of 1% and 2% (F4-TCNQ to polymer ratio) and without F4-TCNQ doping (0%) were spin-coated onto the front surface of the sc-Si wafer at 1500 rpm/s for 30 s to form a continuous P3HT:PCBM:F4-TCNQ films with ∼ 100 nm in thickness. Subsequently, the samples were thermally annealed on the hot plate at 150 °C for 15 min to evaporate the solvents and, simultaneously, to dry the samples. After the spin coating of organic layer, circular-shape gold (Au) rectifying contacts with 99.999% purity in a diameter of 1 mm were evaporated on the P3HT:PCBM:F4-TCNQ organic layer (in front of the Si wafer) through a metal shadow mask by a thermal evaporator vacuum system with a pressure of $\sim 1 \times 10^{-6}$ mbar (1 bar = 10^5 Pa). The thickness of circular-shape Au contacts and the deposition rate of the Au evaporation were ∼ 2500 Å and ∼ 3 Å/s, respectively, and both were monitored by the digital quartz crystal thickness monitor. It should be noticed that the diode preparation procedures were kept the same as those of the corresponding diodes for accurate comparison.

2.3. Schottky barrier diode characterization

The current–voltage (I–V) characteristics of the Au/P3HT:PCBM:F4-TCNQ/n-Si SBDs with different F4-TCNQ concentrations, i.e. 0%, 1%, and 2%, were determined by using a Keithley 4200 SCS separately in the dark and at room temperature. Moreover, IEEE-488 AC/DC converter card connected to computer was used for I–V measurements. The I–V characteristics were determined for many Au rectifying contacts in one device, however, the performance parameters of the best contact in that device were considered. All measurements were carried out immediately after preparation of the SBDs to avoid any change in the electrical characteristic caused by aging, contamination, and interaction with air.

3. Results and discussion

The forward and reverse bias current–voltage ($\ln I$–V) characteristics of the Au/P3HT:PCBM:F4-TCNQ/n-Si (MPS) SBDs in the dark and at room temperature are shown in Fig. 1 for the three different F4-TCNQ concentrations, i.e. 0%, 1%, and 2%. In Fig. 1, the weak voltage dependence of the current in the reverse bias region and the exponential increase of the current in the forward bias region are the characteristic properties of rectifying contacts. As shown in Fig. 1, the I–V characteristics of MPS SBDs are nonlinear and asymmetric and show good rectification behavior with very small leakage current and a potential barrier at the interface, which is characteristic for thermionic emission (TE) current.[25] Additionally, this behavior of the I–V curve is the occurring of a Schottky barrier for each of all diodes independent of F4-TCNQ concentration. For Schottky structure, the presence of interface state, the value of series resistance and ideality factor greater than unity ($n > 1$) give rise to the nonlinear I–V characteristics. By considering these effects and according to TE ($V \geq 3kT/q$) model, the current–voltage relation for the Au/P3HT:PCBM:F4-TCNQ/n-Si (MPS) SBDs can be expressed as[25,26]

$$I = I_0 \left[\exp\left(\frac{q(V - IR_s)}{nkT} \right) - 1 \right], \tag{1}$$

where

$$I_0 = AA^* T^2 \exp\left(-\frac{q\Phi_{B0}}{kT} \right) \tag{2}$$

is the reverse saturation current derived from the straight line intercept of $\ln I$–V plot at $V = 0$, V is the definite forward bias voltage, IR_s is the voltage drop across the R_s (series resistance) of diode, k is the Boltzmann constant, T is the absolute temperature in Kelvin, q is the electronic charge and n is the ideality factor. Additionally, A is the rectifier contact area, A^* is

the effective Richardson constant (equal to 120 $A\cdot cm^{-2}\cdot K^{-2}$ for n-type Si[26,27]) and Φ_{B0} is the apparent barrier height at zero bias, which can be extracted from the extrapolated I_0 and written as the following relation:

$$\Phi_{B0} = \frac{kT}{q} \ln\left(\frac{AA^*T^2}{I_0}\right). \quad (3)$$

The deviation of practical diode from ideal TE theory can be identified by using ideality factor (n) which can be obtained from the slope of the linear region of the $\ln I$–V plot through the following relation:

$$n = \frac{q}{kT} \frac{d(V - IR_s)}{d(\ln I)}. \quad (4)$$

The forward and reverse bias semilogarithmic I–V curves of the Au/P3HT:PCBM:F4-TCNQ/n-Si (MPS) SBDs with different F4-TCNQ concentrations of 0%, 1%, and 2% in the dark and at room temperature are given in Fig. 1. The applied voltage is varied from −5.0 V to +5.0 V in I–V measurements. As can be seen in Fig. 1, the forward bias semilogarithmic $\ln I$–V plot for each of all diodes has a linear region in low voltage region and a considerable deviation from linearity in high enough voltage region especially due to the effect of R_s and interfacial polymer layer. Additionally, the slope of the linear portion of the forward bias $\ln I$–V plot changes with F4-TCNQ concentration, which results in different n values for different F4-TCNQ concentrations. Moreover, the soft non-saturation behavior is observed as a function of applied bias voltage in the reverse bias region, which may be explained in terms of the image-force lowering of Schottky barrier height (SBH) and the existence of P3HT:PCBM:F4-TCNQ organic layer at M/S interface.[28] Additionally, from Fig. 1, the I–V characteristics of all MPS SBDs each have a good rectifying behavior with a potential barrier at the interface between n-Si and P3HT:PCBM:F4-TCNQ organic layer. The rectification behavior can be analyzed by the rectification ratio (RR). The value of RR can be defined as a ratio of the forward to reverse bias current at a fixed voltage (±5 V). The values of RR for Au/P3HT:PCBM:F4-TCNQ/n-Si (MPS) SBDs with F4-TCNQ concentrations of 0%, 1%, and 2% are 0.2×10^3, 4.2×10^3, and 0.4×10^3, respectively. The highest rectification ratio, which is quite important for a broad spectrum of electronic applications,[29] is achieved in the case of soft F4-TCNQ doping (1%). The magnitude of rectification ratio of the diode with 1% F4-TCNQ doping concentration is almost 10 times higher than that of the diode with 2% F4-TCNQ doping concentration. Moreover, more than 20 times higher rectification ratio appears in the diode with 1% F4-TCNQ doping concentration than that in the diode without F4-TCNQ doping (0%). The 1% F4-TCNQ doping of diode reduces the dark current under reverse bias and leads to lower leakage current at zero bias, resulting in higher rectification ratio. Furthermore, the polaron or bipolaron band in forbidden energy gap accompanied by a downward shifted Fermi level (work function) can be created by 1% F4-TCNQ-doping in P3HT:PCBM interfacial organic layer. The 1% F4-TCNQ doped interfacial organic layer with downward shifted Fermi level is utilized for correcting holes and reducing the accumulation of generated carriers. This may reduce the electron–hole recombination loss and leakage current for the diode with 1% F4-TCNQ doping. Additionally, it can be concluded that the diode with 1% F4-TCNQ allows high charge injection through the organic layer under forward bias, much less under reverse bias. It can be assumed that the structures and the morphologies of films are changed by using the different F4-TCNQ concentrations (0%, 1%, and 2%),[19] which affects the properties of the SBD. Additionally, the hole injection is improved by reducing the injection barrier height upon doping explained by the presence of an F4-TCNQ doping in interfacial organic layer.[21] However, the root-mean-square (RMS) value of Au/P3HT:PCBM:F4-TCNQ/n-Si structure increases dramatically with the addition of F4-TCNQ.[19] Therefore, the highly doped (2%) sample with more rough surface shows lower RR than that the diode with a 1% F4-TCNQ.

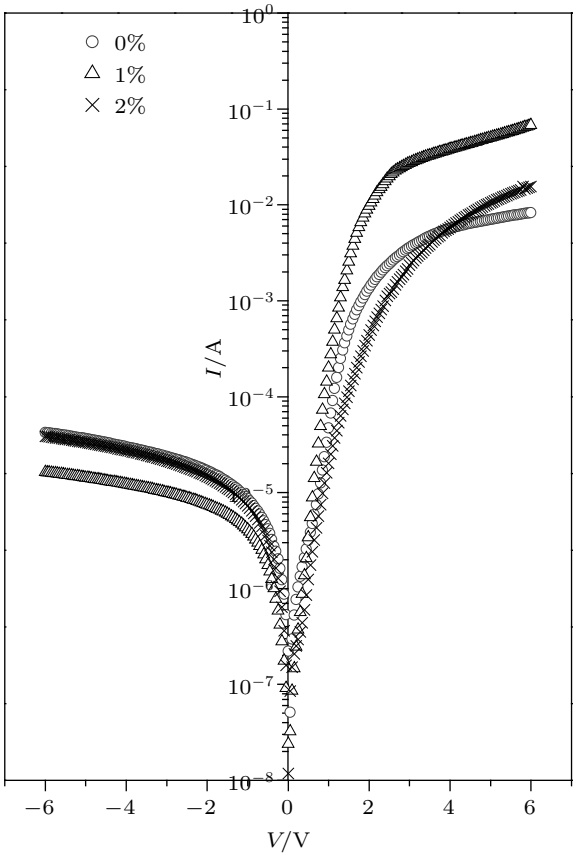


Fig. 1. Forward and reverse bias I–V characteristics of the Au/P3HT:PCBM:F4-TCNQ/n-Si (MPS) SBDs doped respectively with 0%, 1%, and 2% F4-TCNQ concentrations.

By fitting the linear region of the forward bias $\ln I$–V characteristics (Fig. 1) using the TE model, the values of Φ_{B0} and

n for the Au/P3HT:PCBM:F4-TCNQ/n-Si (MPS) SBD dependent on F4-TCNQ concentration are determined from the y-intercept and the slope of the fitted curve, respectively. Additionally, the value of I_0 for MPS SBD are derived from the straight line intercept of $\ln I$–V plot $V = 0$ in Fig. 1 by using Eq. (2). The calculated values of Φ_{B0}, n, and I_0 are reported in Table 1. As can be seen in Table 1, the concentration of F4-TCNQ has a great influence on the values of diode parameters of Φ_{B0}, n, and I_0, which are improved by the F4-TCNQ doping. The results listed in Table 1 show that all SBDs are nonideal diodes due to higher value of n ideality factor than unity ($n > 1$). The higher value of n can be attributed to the high density of N_{ss} localized at metal/polymer (M/P) interface, high value of R_s, the effect of barrier inhomogeneity, recombination of electrons and holes in depletion region and existence of tunneling.[30,31] Additionally, the higher n value may be due to the relatively large voltage drop in metal–polymer (M/P) interface region. On the other hand, it is noted that the value of barrier height, which is the contact potential barrier and exists at the interface between the organic layer and metals, decreases from 0.77 eV to 0.71 eV with 1% F4-TCNQ doping and becomes almost the same with 2% F4-TCNQ doping as with no doping. The P3HT:PCBM:F4-TCNQ organic blends with different F4-TCNQ concentrations modify the interfacial electrical parameters of the Au/P3HT:PCBM:F4-TCNQ/n-Si (MPS) SBDs and affect the space charge regions of the SBDs by changing the values of Φ_{B0}. Additionally, F4-TCNQ with 1% concentration yields the lower barrier height with lower series resistance. So, current flow becomes higher for the 1% F4-TCNQ diode with lower barrier height, which is because only electrons with energy above the barrier will contribute to the forward current.[25] As a result, current will flow through patches of the lower barrier height, hence, giving lower ideality factor value. Moreover, the improvement of basic electrical parameters dependent on F4-TCNQ doping can be concluded that the conductivity of MPS SBD increases dramatically with F4-TCNQ doping, since the doping of semiconductor leads to the enhancement of the electric field at the metal/semiconductor interface which gives rise to a reduction in the injection barrier due to the image force lowering. On the other hand, the value of I_0 increases ~ 10 times by adding the 1% F4-TCNQ, whereas the values of n and Φ_{B0} become lower. However, the values of n and Φ_{B0} increase, while I_0 decreases for the diode doped with a 2% F4-TCNQ concentration when compared with the diode doped with a 1% F4-TCNQ concentration. The electrical parameters are enhanced in the case of soft F4-TCNQ doping (1%), while hard doping (2%) negatively affects the electrical parameters of SBD. This is probably due to unbalanced generation of holes/electrons and doping-induced disproportion when more F4-TCNQ is added. Additionally, the high doping generally produces hole trapping side, which reduces the conductivity and the electrical properties of diode. Moreover, the decrease in basic parameter by using 2% F4-TCNQ can be due to the enhancement in surface roughness with the hard doping of F4-TCNQ.[19] The much smoother device surface of soft F4-TCNQ doping (1%) diode may lead to better interfacial contact with the top electrode by resulting in higher current flow.

The parasitic resistances, which are the series resistance R_s and the shunt resistance R_{sh}, affect the I–V characteristics of the SBD. The mechanism of the diode can be understood by determining the values of R_s and R_{sh}, while the performance of the SBD can be determined by these parasitic resistances. Shunt resistance is associated with the polymer/semiconductor (P/S) interface. However, the series resistance is related to metal/polymer (M/P) interface properties. In an ideal diode, the value of R_s should be low (≈ 0) whereas R_{sh} value is quite high (megaohms). The R_{sh} of diode can be calculated by using the equation of $R_{sh} = (\partial V/\partial I)|_{V=0}$ and is described as the dynamic resistance at the origin.[32] The R_{sh} appears from the leakage of the current. The R_s of a diode can be defined as the sum of the total resistance of the ohmic contacts and the resistance of the undepleted semiconductor bulk. The values of R_s and R_{sh} describe the SBD resistance (R_i) in forward bias and reverse bias, respectively. For an ideal diode, $R_i (= \partial V/\partial I)$ approaches to zero by increasing the forward voltage. However, the generation and recombination of the carriers in the depletion region, high-injection conditions and imperfect ohmic contacts can significantly change the forward current. The values of R_s and R_{sh} can be determined by using the R_i versus V plot which is shown in Fig. 2, indicating that they are dependent on F4-TCNQ doping concentration for the Au/P3HT:PCBM:F4-TCNQ /n-Si (MPS) SBDs. As shown in Fig. 2, the values of R_s and R_{sh} for all samples approach to their constant values in forward bias region and reverse bias region, respectively. The values of R_s are 427.1 Ω, 46.1 Ω, and 197.4 Ω, while the values of R_{sh} are 0.2 MΩ, 0.7 MΩ, and 0.4 MΩ for 0%, 1%, and 2% F4-TCNQ doping SBDs, respectively. The lowest R_s and the highest R_{sh}, which indicate the more ideal diode, are obtained for 1% F4-TCNQ diode.

Table 1. The experimental values of diode parameters calculated by various methods from the forward bias I–V characteristics of different F4-TCNQ doping concentrations-doped Au/P3HT:PCBM:F4-TCNQ/n-Si (MPS) SBDs.

Doping concentrations	From $\ln I$–V			From $H(I)$–I		From $dV/d(\ln I)$–I		From $F(V)$–V	
	n	I_0/A	Φ_{B0}/eV	R_s/Ω	Φ_{B0}/eV	R_s/Ω	n	Φ_B/eV	R_s/Ω
0%	7.53	1.18×10^{-8}	0.77	380.5	0.76	380.5	8.73	0.81	394.0
1%	4.70	1.16×10^{-7}	0.71	46.96	0.72	44.3	6.68	0.77	54.4
2%	6.49	2.08×10^{-8}	0.75	183.4	0.74	183.7	7.72	0.79	157.9

The decrease in R_s and increase in R_{sh} by F4-TCNQ doping are quite compatible with the above discussion about Φ_{B0}, n, and I_0. This means that the Au/P3HT:PCBM:F4-TCNQ/n-Si (MPS) SBDs turns close to more ideal diode with the lower R_s and higher R_{sh} by F4-TCNQ doping. Additionally, it can be concluded that R_s and R_{sh} are both strong functions of the applied voltage and the doping of organic interfacial layer. Moreover, electron transfer from the HOMO of the conjugated organic structure to the LUMO of the dopant molecules may lead to a gradual shift of the organic Fermi level towards its HOMO level. This reduces the interface injection barrier by increasing the conductivity, i.e. reducing the R_s, with F4-TCNQ doping. Additionally, the hole injection is improved by tunneling the Fermi level of the polymer. However, the value of R_s becomes higher by increasing the doping concentration (2%). It can be due to the formation of insulating layer between the active layer and anode, which may charge blocking layer resulting in larger R_s, with increasing doping concentration.

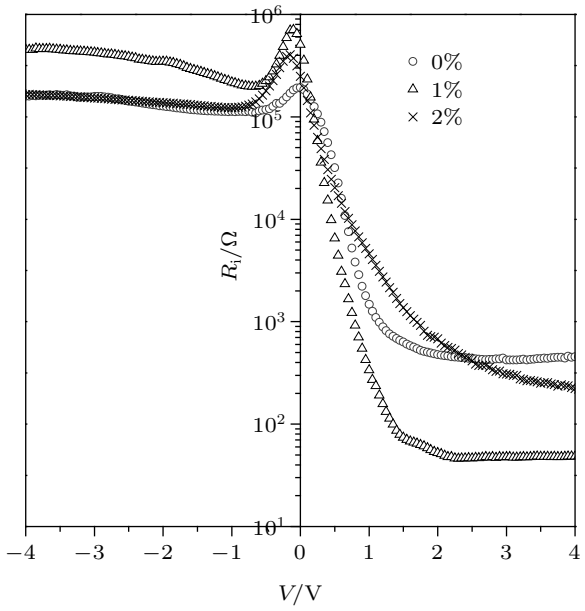


Fig. 2. The plots of SBD resistance (R_i) versus applied bias voltage for Au/P3HT:PCBM:F4-TCNQ/n-Si (MPS) SBDs doped respectively with 0%, 1%, and 2% F4-TCNQ doping concentrations.

The dominant current conduction mechanism of the Au/P3HT:PCBM:F4-TCNQ/n-Si (MPS) SBD as a function of F4-TCNQ doping concentration can be analyzed by the double logarithmic I–V plot at room temperature as shown in Fig. 3. As depicted in Fig. 3, three distinct linear regions representing different current conduction mechanisms independent of F4-TCNQ concentration can be identified. Each linear region has different slopes for each of all samples. In these regions, the current is directly proportional to the applied voltage as $I \propto V^m$, where m is the slope of each linear region and determines the conduction mechanisms.[33,34] As shown in Fig. 3, the current is linearly proportional to the voltage ($I \propto V$) at low applied voltages (< 0.3 V). This corresponds to the ohmic conduction, which implies that the density of thermally generated free electrons inside the films is larger than the injected carriers, at low voltage region (< 0.3 V) independent of F4-TCNQ doping concentration. The current increases rapidly when the applied voltage reaches a certain threshold voltage (V_{th}). The current varies with applied voltage as $I \propto V^m$ with $m > 2$ in voltage range from 0.3 V to 2.0 V for all samples. Therefore, the conduction mechanism of current is changed into the trap-controlled space-charge limited current (SCLC) conduction in a medium voltage range from 0.3 V to 2.0 V. The presence of SCLC shows that at least one contact has good injecting properties to provide an inexhaustible carrier source. With the rise in voltage ($V_{bias} \geq 0.3$ V), density of injected carriers from electrodes as response to an applied voltage increase, which dominates the charge carrier transport capacity of organic blended layer and fills up the traps. SCLC conduction mechanism is the results of current which is limited when applied electric field is dominated by the field due to space charge. SCLC mechanism appears when the bulk relaxation time exceeds the transit time of any excess injected carrier.[35] The interaction of the carriers with localized defect state can be designated by both the magnitudes of the current response and the actual form of I–V characteristics. When the applied voltage is high enough (> 2.0 V), the slope becomes close to 2 ($I \propto V^2$) for each of all samples and indicates the trap-free square-law region, while the region with $m > 2$ corresponds to the trap-filled-limit region (TFL). The Fermi level moves up above the electron trapping level by increasing the applied voltage which leads to the enhancement in the density of free carriers from injection.[36] TFL is the condition for the transition from the trapped I–V characteristics to the trap-free I–V characteristics. It can be envisioned that the injected carriers will be free to move in the organic films after all traps have been filled up, so that the current will rapidly jump from its low trap-limited value to a high trap-free SCLC. As can be seen in Fig. 3, the value of m is higher for the diode doped with 1% F4-TCNQ concentration in a voltage range from 0.3 V to 2.0 V than for other diodes. This can be attributed to the decrease of the irregularity of the polymer film by using the 1% F4-TCNQ doping for the Au/P3HT:PCBM:F4-TCNQ/n-Si (MPS) SBD, which may lead to higher mobility and diffusion of the carriers in the polymer matrix.[37] In organic semiconductors, charge carrier mobility is not high enough to sweep extra-injected charges to the receiving electrode.[35] The I–V behavior shown in Fig. 3 can be modeled in terms of the SCLC mechanism. The electron mobility can be determined from $\ln I$–$\ln V$ curve for the Au/P3HT:PCBM:F4-TCNQ/n-Si (MPS) SBD using SCLC model at medium voltages of 0.3 V–2.0 V. Therefore, the space charge-limited current can be given by[36]

$$I = \frac{9}{8}\varepsilon_0\varepsilon_s\mu_e\frac{A}{d^3}V^2, \tag{5}$$

where ε_0 is the permittivity of free space, ε_s is the permittivity of semiconductor, d is the thickness of interfacial organic layer ($\sim$ 100 nm for each of all samples, measured by use of a Dektak step profilometer), and μ_e is the mobility of the electron in interfacial organic layer. In Eq. (5), the effect of traps on the charge transport is ignored since all the traps are filled. The values of μ_e were found to be 3.88×10^{-5} $m^2 \cdot V^{-1} \cdot s^{-1}$, 6.71×10^{-5} $m^2 \cdot V^{-1} \cdot s^{-1}$, and 6.07×10^{-5} $m^2 \cdot V^{-1} \cdot s^{-1}$ for 0%, 1%, and 2% F4-TCNQ SBDs, respectively. These mobility values are quite compatible with such organic semiconductors.[38,39] According to mobility results, the electron mobility increases from 3.88×10^{-5} $m^2 \cdot V^{-1} \cdot s^{-1}$ (0%) to 6.71×10^{-5} $m^2 \cdot V^{-1} \cdot s^{-1}$ (1%) by F4-TCNQ doping. It is shown that the mobility of carriers in diode increases by F4-TCNQ doping. The reason for this enhancement can be explained as the fact that the addition of F4-TCNQ doping even in small quantities effectively increases the crystalline order which improves the molecular orientation of P3HT chains. This orientation allows the charge carrier to transport in the two-dimensional conjugation direction, which results in a higher mobility for F4-TCNQ-doped samples.[14] On the other hand, the mobility value of 2% F4-TCNQ diode is slightly lower than that of 1% F4-TCNQ diode, which can be explained to be due to the conductivity lowering with the increase in doping concentration as discussed above.

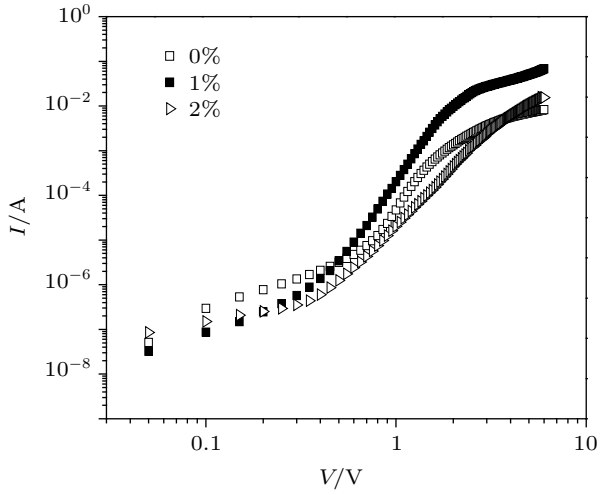


Fig. 3. Double logarithmic I–V characteristics of the Au/P3HT:PCBM:F4-TCNQ/n-Si (MPS) SBDs in the forward bias region at room temperature for 0%, 1%, and 2% F4-TCNQ concentrations in P3HT:PCBM:F4-TCNQ interfacial organic layer.

As seen in Fig. 1, the $\ln I$–V curves of diodes doped with different F4-TCNQ concentrations are all nonlinear. The I–V characteristics independent of F4-TCNQ concentration have two linear regions in forward bias region, one has a high slope value in low bias region and the other has a smaller slope value in high bias region. Such a deviation from linearity of I–V characteristics for the diodes doped with different F4-TCNQ concentrations can be due to the effects of R_s, the organic interfacial layer and the interface states when the applied voltage is high enough. Additionally, voltage dependences of $\Phi_B(V)$ and $n(V)$ can also be the reason for this nonlinear I–V behavior in the forward bias region. The other characterization techniques evaluating the values of R_s, Φ_B, and n were developed by Cheung and Cheung[40] in the nonlinear region of $\ln I$–V curve in the forward bias region. According to Cheung's functions, the thermionic emission model for a Schottky diode having junction resistance at $V > 3kT/q$ in the forward I–V characteristic can be written as[40]

$$\frac{dV}{d(\ln I)} = n\frac{kT}{q} + IR_s, \tag{6}$$

$$H(I) = V - \left(\frac{nkT}{q}\right)\ln\left(\frac{I}{AA^*T^2}\right), \tag{7}$$

and

$$H(I) = IR_s + n\Phi_B. \tag{8}$$

The plots of $dV/d(\ln I)$ versus I and $H(I)$ versus I for 0%, 1%, and 2% for Au/P3HT:PCBM:F4-TCNQ/n-Si (MPS) SBDs with 0%, 1%, and 2% F4-TCNQ concentrations at room temperature are presented in Figs. 4(a)–4(c), respectively. According to Eqs. (6) and (8), the plots of forward bias $dV/d(\ln I)$ versus I and $H(I)$ versus I exhibit linear behaviors for all MPS diodes as depicted in Fig. 4. The R_s and n values are calculated from the slope and y-axis intercept of linear $dV/d(\ln I)$–I plots, respectively, considering Eq. (6). Additionally, the second determination of R_s is determined from the slope of $H(I)$–I plot to inspect the compatibility of Cheung's method. The values of Φ_{B0} are obtained from the y-axis intercept of $H(I)$–I curve plotted using Eq. (8). The values of R_s, n, and Φ_{B0} derived from the analysis of $dV/d(\ln I)$–I and $H(I)$–I plots for 0%, 1%, and 2% F4-TCNQ MPS diodes are listed in Table 1. In Table 1, the ideality factor values obtained from the downward curvature regions of forward bias I–V plots (i.e., $dV/d(\ln I)$–I plots) and from the linear regions of the same characteristics (i.e., $\ln I$–V plots) are different from each other. The values of n determined from the forward bias $\ln I$–V plots are lower than n values deduced from $dV/d(\ln I)$–I plots. This may be due to the bias dependence of Schottky barrier height according to the voltage drop across the interfacial layer and the change of the interface states with the bias in the low-voltage region of the current–voltage plot and the series resistance.[41] Additionally, the interface dipoles and fabrication-induced defects at the interface as well as the presence of the P3HT:PCBM:F4-TCNQ organic layer can be the other effects responsible for the differences among these ideality factor values. As can be seen in Table 1, the R_s values obtained from the Cheung functions are almost the same, which can be ascribed to the consistency of Cheung functions. Moreover, the values of Φ_{B0} deduced from Cheung's method are in good agreement with the values of Φ_{B0}, derived from the I–V characteristics, which are independent of the F4-TCNQ

doping concentration value. On the other hand, considerable attention should be paid to the values of n, R_s, and Φ_{B0} each as a function of F4-TCNQ concentration in P3HT:PCBM:F4-TCNQ interfacial organic layer. This may be due to the F4-TCNQ doping of P3HT:PCBM interfacial organic blend layer which modifies the barrier height by influencing the space charge region of the Au/P3HT:PCBM:F4-TCNQ/n-Si (MPS) SBD. Additionally, the lower n, lower R_s, and lower Φ_{B0} were obtained for the diode doped with 1% F4-TCNQ by Cheung method as well as I–V method, owing to the enhancement in conductivity and charge mobility by using the 1% dopant concentration.

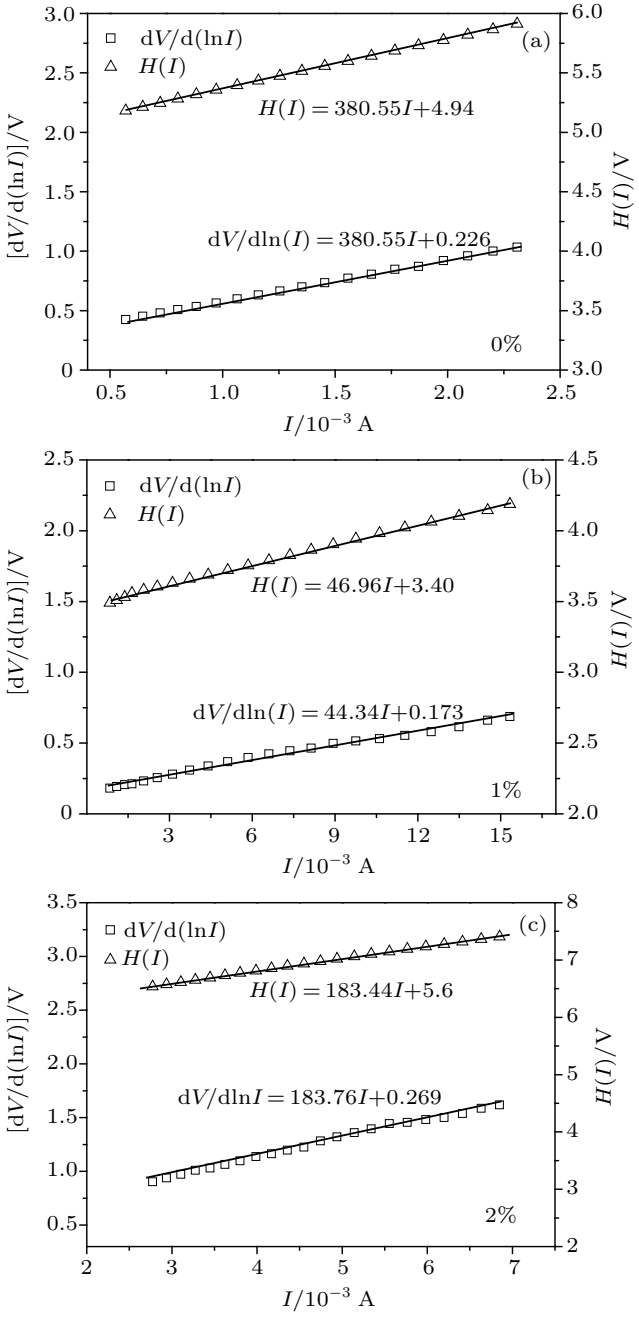


Fig. 4. Experimental $dV/d(\ln I)$ and $H(I)$ versus I plots for (a) 0%, (b) 1%, and (c) 2% F4-TCNQ concentration-doped Au/P3HT:PCBM:F4-TCNQ/n-Si (MPS) SBDs in dark at room temperature.

By including the effect of the high series resistance and higher ideality factor than unity ($n > 1$), the barrier height can be accurately determined through using the Norde method which is given below[42]

$$F(V) = \frac{V}{\gamma} - \frac{kT}{q}\ln\left(\frac{I(V)}{AA^*T^2}\right), \tag{9}$$

where γ is an arbitrary integer (dimensionless) greater than the value of ideality factor n deduced from I–V characteristics and $I(V)$ is the current profile depending on V. The junction parameters Φ_B and R_s are also determined by using Norde method for the Au/P3HT:PCBM:F4-TCNQ/n-Si (MPS) SBDs with different F4-TCNQ concentrations. Firstly, $F(V)$ versus V shown in Fig. 5 is plotted by using Eq. (9). Then, the value of barrier height Φ_B is calculated from the following expression:

$$\Phi_B = F(V_0) + \frac{V_0}{\gamma} - \frac{kT}{q}, \tag{10}$$

where $F(V_0)$ is the least value of $F(V)$ and V_0 is the corresponding voltage value. The value of R_s is determined from the Norde's method as

$$R_s = \frac{kT(\gamma - n)}{qI_0}, \tag{11}$$

where I_0 is the current value corresponding to the minimum point of $F(V_0)$ at the lowest voltage. The approach given in Eq. (11) is valid only for high-value R_s.[43] When the lowest position of $F(V)$, i.e. $F(V_0)$, at $V = V_0$ is found, the values of Φ_B and R_s for F4-TCNQ dopant concentration-dependent Au/P3HT:PCBM:F4-TCNQ/n-Si (MPS) SBDs at room temperature are calculated as given in Table 1. The results show that the values of Φ_B and R_s, calculated from Cheung functions and Norde's technique are in good agreement with each other (Table 1). On the other hand, it is noted that these values of R_s are higher than those obtained by the I–V method, and independent of doping concentration. This means that the series resistance is a current-limiting factor for the Au/P3HT:PCBM:F4-TCNQ/n-Si (MPS) SBD. The effect

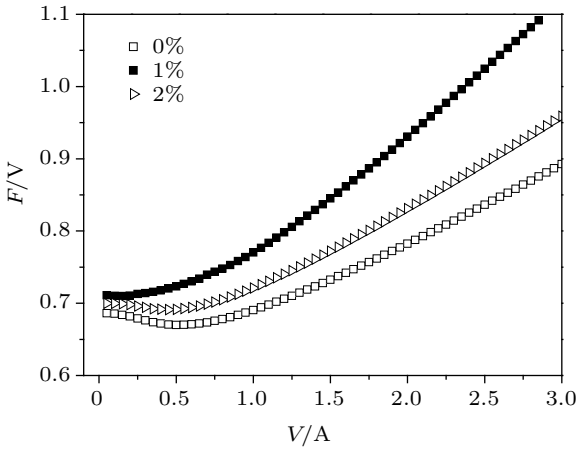


Fig. 5. $F(V)$ versus V plots for the Au/P3HT:PCBM:F4-TCNQ/n-Si (MPS) SBDs doped respectively with F4-TCNQ concentrations of 0%, 1%, and 2%.

of R_s is usually modeled as a series combination of a diode and a resistance. The voltage drop across a diode is determined in terms of the total voltage drop across the diode and the resistance.[44] Furthermore, the values of Φ_B obtained from Norde function for all samples are slightly higher than those obtained from Cheung functions. It can be explained as the fact that Cheung functions are only applicable to the nonlinear region in high voltage region of the forward-bias $\ln I$–V characteristics, while Norde's function is applicable to the full forward bias region of the $\ln I$–V characteristics.

The density of interface states (N_{ss}) is quite important for designating the quality of MPS SBDs. As discussed above, the ideality factor n becomes greater than unity due to the effect of interface state in equilibrium with semiconductor. However, there is no study in literature about the effect of F4-TCNQ doping concentration in the interface states of the Au/P3HT:PCBM:F4-TCNQ/n-Si (MPS) SBDs. The density distribution curve of the interface state N_{ss} can be determined from the forward bias $\ln I$–V characteristic shown in Fig. 1. For Au/P3HT:PCBM:F4-TCNQ/n-Si (MPS) SBDs, the ideality factor becomes the voltage-dependent ($n(V)$) due to either nonlinear behavior of I–V curve or the presence of the P3HT:PCBM:F4-TCNQ interfacial organic layer and R_s as expressed by the following equation[31]

$$n(V) = \frac{q}{kT}\frac{(V - IR_s)}{\ln(I/I_0)}. \tag{12}$$

Due to the nonideal I–V characteristics of MPS SBDs, n becomes N_{ss}-dependent and greater than unity ($n > 1$) as deduced by Card and Rhoderick.[31] By considering these effects, voltage-dependent n can be given by[31,45]

$$n(V) = 1 + \frac{d}{\varepsilon_i}\left[\frac{\varepsilon_s}{W_D} + qN_{ss}(V)\right], \tag{13}$$

where d is the thickness of interfacial organic layer, W_D is the width of the space charge region calculated from the experimental C^{-2} versus V plot at 1 MHz, ε_i ($= 3.8\varepsilon_0$) and ε_s ($= 11.8\varepsilon_0$) are the permittivities of the interfacial and the semiconductor layer, respectively. According to Eq. (13), the density of the interface states N_{ss} can be written as

$$N_{ss} = \frac{1}{q}\left[\frac{\varepsilon_i}{d}(n(V) - 1) - \frac{\varepsilon_s}{W_d}\right]. \tag{14}$$

In n-type semiconductors, the energy of the interface states (E_{ss}) can be defined in terms of the bottom of the conduction band at the semiconductor surface (E_c) through the following relation[31]

$$E_c - E_{ss} = q(\Phi_e - V), \tag{15}$$

where Φ_e is the effective barrier height. The voltage-dependent effective barrier height Φ_e is related to the voltage-dependent ideality factor $n(V)$ by the following expression:

$$\Phi_e = \Phi_{B0} + \beta(V - IR_s) = \Phi_{B0} + \left(1 - \frac{1}{n(V)}\right)(V - IR_s), \tag{16}$$

where β, which combines the effects of N_{ss} and R_s, is the voltage coefficient of the effective barrier height Φ_e.

For diodes doped with 0%, 1%, and 2% F4-TCNQ concentrations, the energy distribution profiles of N_{ss} with and without taking R_s into account are determined from the experimental data of the forward bias I–V characteristics by using Eq. (14) (Eq. (6)). As shown in Fig. 6, the distribution profiles of N_{ss} with and without taking account the R_s have the apparent exponential increase with the increase in applied bias from the midgap towards the bottom of the conduction band of Si for all samples, and they are independent of F4-TCNQ doping concentration. In this case, the acceptor-type N_{ss} is in effect near the valance band, while the donor-type N_{ss} is in effect near the conductance band. The shapes of the density distribution of N_{ss} are in the ranges from $E_c - 0.42$ eV to $E_c - 0.65$ eV for the diode doped with a 0% F4-TCNQ concentration, from $E_c - 0.36$ eV to $E_c - 0.67$ eV for the diode doped with a 1% F4-TCNQ concentration, and from $E_c - 0.40$ eV to $E_c - 0.68$ eV for the diode doped with a 2% F4-TCNQ concentration. Additionally, the results show that the density of N_{ss} strongly depends on the applied bias and increases with the enhancement in the applied bias corresponding to a position inside the Si gap. As shown in Fig. 6, there are differences in the magnitude of the N_{ss} between the cases with and without taking into account the R_s in $E_c - 0.40$ eV for the diodes doped with 0%, 1%, and 2% F4-TCNQ concentrations correspondingly. As seen from Fig. 6, the values of N_{ss} without taking account of the R_s are lower than those calculated by considering the effect of R_s on N_{ss}. These results show that the value of R_s should be considered in the calculation of N_{ss}.

On the other hand, when the effect of F4-TCNQ doping concentration on the N_{ss} profile of the Au/P3HT:PCBM:F4-TCNQ/n-Si (MPS) SBDs is considered in $E_c - 0.45$ eV, the magnitudes of N_{ss} are 1.4×10^{12} eV^{-1}·cm^{-2}, 7.5×10^{11} eV^{-1}·cm^{-2}, and 1.7×10^{12} eV^{-1}·cm^{-2} for the diodes doped with 0%, 1%, and 2% F4-TCNQ concentrations, respectively. N_{ss} value of the diode doped with a 1% F4-TCNQ concentration is almost twice less than that of diode without F4-TCNQ doping (0%). Furthermore, the highest value of N_{ss} is obtained for the diode doped with a 2% F4-TCNQ concentration. This significant decrease of N_{ss} with the F4-TCNQ concentration value of 1% may be due to the lower barrier height at metal/polymer (M/P) interface and increased velocity and mobility of charge carriers for the Au/P3HT:PCBM:F4-TCNQ/n-Si (MPS) SBD with a 1% F4-TCNQ concentration. On the other hand, the increase in F4-TCNQ doping concentration results in higher N_{ss} since high doping level creates additional traps at the M/S interface, which reduces the carrier injection and conductivity.

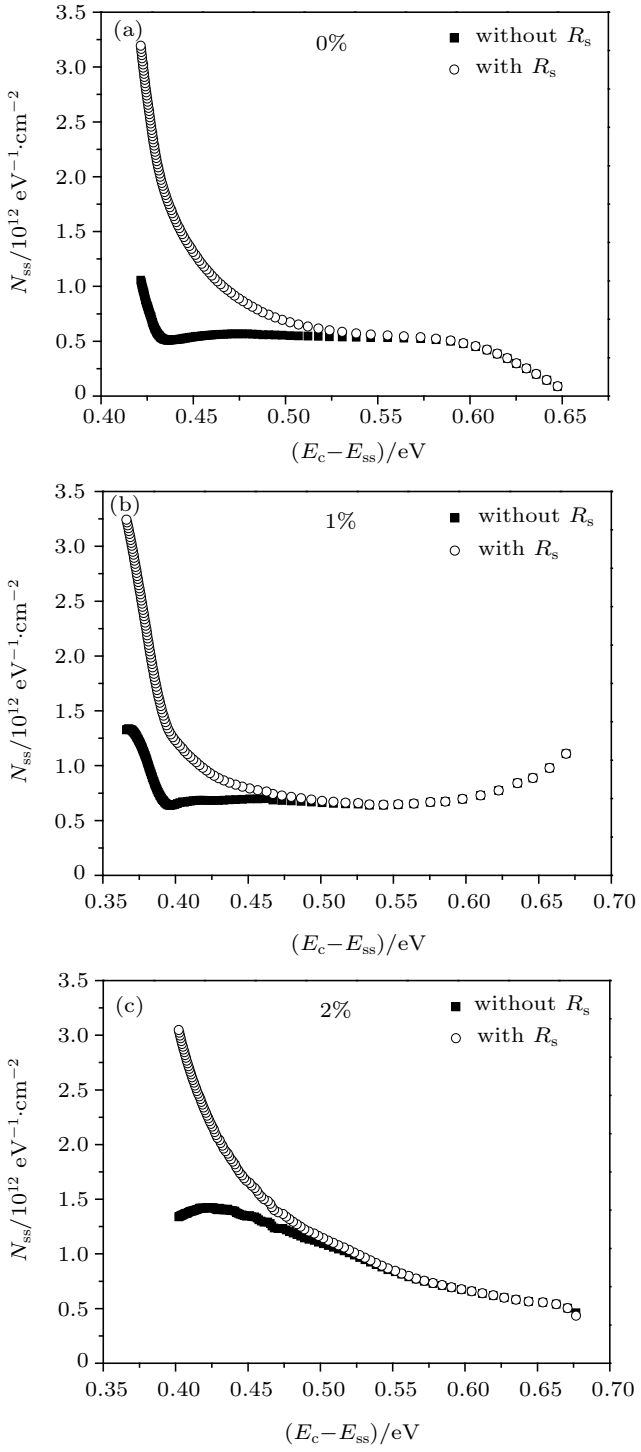


Fig. 6. The interface state energy distribution curves of the Au/P3HT:PCBM:F4-TCNQ/n-Si (MPS) SBDs doped respectively with (a) 0%, (b) 1%, and (c) 2% F4-TCNQ concentrations with and without taking the series resistance into account in the calculations.

4. Conclusions

The Au/P3HT:PCBM:F4-TCNQ/n-Si (MPS) Schottky barrier diodes (SBDs) are fabricated using different F4-TCNQ doping concentration values, i.e., 0%, 1%, and 2%. The forward and reverse bias *I–V* measurements in the dark and at room temperature are used to determine the electrical and interfacial parameters of MPS SBDs dependent on F4-TCNQ doping concentration. The significant enhancement in the rectification ratio by using 1% F4-TCNQ concentration is observed from the ln*I–V* plots when comparing those of undoped and 2% F4-TCNQ-doped MPS diodes. The rectification ratio results show that the different F4-TCNQ doping concentrations, i.e., 0%, 1%, and 2%, in P3HT:PCBM:F4-TCNQ interfacial organic layers give rise to changes in the structures and the morphologies of films, while the diode doped with 1% F4-TCNQ concentration allows the high charge injection through the organic film under forward bias and much less under reverse bias. The basic electrical parameters, such as ideality factor (n), series resistance (R_s), barrier height (Φ_{B0}), and density of interface states (N_{ss}), are determined from the *I–V* characteristics and compared in the cases of different F4-TCNQ doping concentrations (0%, 1%, and 2%). It is found that all basic electrical parameters strongly depend on the F4-TCNQ doping concentration of interfacial organic layer in each Au/P3HT:PCBM:F4-TCNQ/n-Si (MPS) SBD. There are significant improvements of basic electrical parameters by F4-TCNQ doping in the Au/P3HT:PCBM:F4-TCNQ/n-Si (MPS) SBDs, which results in lower ideality factor, higher rectification ratio, lower series resistance, and higher shunt resistance values. The improvement of basic electrical parameters with the doping of F4-TCNQ indicates that the conductivity of MPS SBD increases dramatically with F4-TCNQ doping since the doping of semiconductors leads to the enhancement of the electric field at the metal/semiconductor interface which gives rise to a reduction in the injection barrier due to image force lowering. Additionally, the enhancement in mobility is reduced for 1% F4-TCNQ doped diode. This can be due to the decrease of the irregularity of the polymer film and the diffusion of more carriers in the polymer matrix by increasing the F4-TCNQ concentration. Additionally, all electrical parameters can be considerably improved in the case of soft F4-TCNQ doping (1%), while hard doping (2%) slightly improves the diode parameters compared with undoping. This is probably due to unbalanced generation of holes/electrons and doping-induced disproportion when more F4-TCNQ is added. Additionally, highly doping generally produces hole trapping side, which reduces the conductivity and the electrical properties of diode. The main electrical parameters are calculated by using different methods, such as ln*I–V* plot, Cheung's method and Norde method. It is found that the values of electrical parameters deduced from the different methods are in good agreement. Moreover, the decrease of N_{ss} with 1% F4-TCNQ doping is obtained. This may be due to the lower barrier height at metal/polymer (M/P) interface and the increased velocity and mobility of charge carriers for 1% F4-TCNQ-doped MPS SBD. On the other hand, the increase in F4-TCNQ doping concentration results in higher N_{ss} since high doping level creates additional traps at M/S interface, which reduces

the carrier injection and conductivity. Finally, it can be concluded that the soft F4-TCNQ doping concentration (1%) of P3HT:PCBM:F4-TCNQ interfacial organic layer significantly improves the quality of the Au/P3HT:PCBM:F4-TCNQ/n-Si (MPS) SBDs.

References

[1] Zhang F, Sun B, Song T, Zhu X and Lee S 2011 *Chem. Mater.* **23** 2084
[2] Lin Y Y, Gundlach D J, Nelson S F and Jackson T N 1997 *IEEE Trans. Electron. Dev.* **44** 1325
[3] Unni K N N, Pandey A K, Alem A and Nunzi J M 2006 *Chem. Phys. Lett.* **421** 554
[4] Burroughes J H, Bradley D D C, Brown A R, Marks R N, Mackay K, Friend R H, Burns P L and Holmes A B 1990 *Nature* **347** 539
[5] Kumar P, Jain S C, Misra A, Kamalasanan M N and Kumar V 2006 *J. Appl. Phys.* **100** 114506
[6] Wu H R, Song Q L, Wang M L, Li F Y, Yang H, Wu Y, Huang C H, Ding X M and Hou X Y 2007 *Thin Solid Films* **515** 8050
[7] Narayan K S, Manoj A G, Singh T B and Alagiriswamy A A 2002 *Thin Solid Films* **417** 75
[8] Pecchia A and Di Carlo A 2004 *Rep. Prog. Phys.* **67** 1497
[9] Onganer Y, Sağlam M, Türüt A, Efeoğlu H and Tüzemen S 1996 *Solid State Electron.* **39** 677
[10] Yu G, Gao J, Hummelen J C, Wudi F and Heeger A J 1995 *Science* **270** 1789
[11] Schilinsky P, Waldauf C and Brabec C J 2002 *Appl. Phys. Lett.* **81** 3885
[12] Song T, Lee S T and Sun B 2012 *J. Mater. Chem.* **22** 4216
[13] Kim J Y, Lee K, Coates N E, Moses D, Nguyen T Q, Dante M and Heeger A J 2007 *Science* **317** 222
[14] Burkhard G F, Hoke E T, Scully S R and McGehee M D 2009 *Nano Lett.* **9** 4037
[15] Liang M A 2010 *Chin. Phys. Lett.* **27** 117301
[16] Chan C K, Zhao W, Kahn A and Hill I G 2009 *Appl. Phys. Lett.* **94** 203306
[17] Zhang Y and Blom P W M 2010 *Appl. Phys. Lett.* **97** 083303
[18] Harada K, Riede M, Leo K and Hild O R 2008 *Phys. Rev. B* **77** 195212
[19] Han X, Wu Z and Sun B 2013 *Org. Electron.* **14** 1116
[20] Aziz E F, Vollmer A, Eisebitt S, Eberhardt W, Pingel P, Neher D and Koch N 2007 *Adv. Mater.* **19** 3257
[21] Lei X, Zhang F, Song T and Sun B 2011 *Appl. Phys. Lett.* **99** 233305
[22] Drees M, Premaratne K, Graupner W, Heflin J R, Davis R M, Marciu D and Miller M 2002 *Appl. Phys. Lett.* **81** 4607
[23] Zhang Y and Blom P W M 2010 *Org. Electron.* **11** 1261
[24] Reinhardt K and Kern W 2008 *Handbook of Silicon Wafer Cleaning Technology* (2nd edn.) (New York: William Andrew Publishing)
[25] Sze S M 1981 *Physics of Semiconductor Devices* (2nd edn.) (New York: Wiley)
[26] Rhoderick E H and Williams R H 1988 *Metal–Semiconductor Contacts* (Oxford: Clarendon Press)
[27] Gökçen M, Tunç T, Altındal Ş and Uslu İ 2012 *Curr. Appl. Phys.* **12** 525
[28] Kampen T U, Park S and Zahn D R T 2002 *Appl. Surf. Sci.* **190** 461
[29] Braun D and Heeger A J 1991 *Appl. Phys. Lett.* **58** 1982
[30] Fang Y, Chen S A and Chu M L 1992 *Synth. Met.* **52** 261
[31] Card H C and Rhoderick E H 1971 *J. Phys. D* **4** 1589
[32] Tabbert B and Goushcha A 2012 *Optical Detectors*, in: *Springer Handbook of Lasers and Optics*, Ed. Träger F (Berlin, Heidelberg, New York: Springer-Verlag) pp. 503–562
[33] Leeuw D M and Lous E J 1994 *Synth. Met.* **65** 45
[34] Yakuphanoglu F, Shah M and Farooq W A 2011 *Acta Phys. Pol. A* **120** 558
[35] Abkowitz M, Facci J S and Rehm J 1998 *J. Appl. Phys.* **83** 2670
[36] Chiu F C 2014 *Adv. Mater. Sci. Eng.* **2014** 578168
[37] John J, Sivaraman S, Jayalekshmy S and Anantharaman M R 2010 *J. Phys. Chem. Solid* **71** 935
[38] Yakuphanoglu F 2007 *Synth. Met.* **157** 859
[39] Gundlach D J, Pernstich K P, Wilckens G, Gruter M, Haas S and Batlogg B 2005 *J. Appl. Phys.* **98** 064502
[40] Cheung S K and Cheung N W 1986 *Appl. Phys. Lett.* **49** 85
[41] Padma R and Reddy V R 2014 *Adv. Mater. Lett.* **5** 31
[42] Norde H 1979 *J. Appl. Phys.* **50** 5052
[43] Prokopyev A I and Mesheryakov S A 2003 *Measurement* **33** 135
[44] Reddy M S P, Kwon M K, Kang H S, Kim D S, Lee J H, Reddy V R and Jang J S 2013 *J. Semicond. Sci. Tech.* **13** 492
[45] Demirezen S, Sönmez Z, Aydemir U and Altındal Ş 2012 *Curr. Appl. Phys.* **12** 266